Research Article

The remarkably improved filler dispersion and performance of SSBR/BR by core–shell structure SiO_2@LDH nanocomposites

Hong Zhu[1] · Xidai Huang[1] · Zhongying Wang[1] · Linghan Kong[1] · Minglin Chen[1] · Fanghui Wang[1]

Abstract
Core–shell structure of SiO_2@MgAl-layered double hydroxide (SiO_2@LDH) as a novel filler was prepared and incorporated into solution-polymerized styrene butadiene rubber/butadiene rubber (SSBR/BR) matrix to prepare SiO_2@LDH–SSBR/BR composites. The results revealed the advanced structure of SiO_2@LDH in the application of elastomer and the strongly interaction between SiO_2 and LDH. The investigation of the fracture surface scanning and the study of 'Payne effect' to the SSBR/BR compounds indicated a good dispersity of filler in the rubber matrix. In addition, the SiO_2@LDH–SSBR/BR composites showed an increased modulus (300% strain) and a decreased modulus (100% strain) compared with commercialized Zeosil 1165MP highly-dispersed SiO_2 nanoparticles. The synergistic enhancement of SiO_2 and LDH in rubber matrix was discussed. The remarkable comprehensive properties enhancement of all the SiO_2@LDH–SSBR/BR was obviously observed in the dynamic mechanical analysis compared with the SiO_2–SSBR/BR samples. The results in this study strongly illustrate that SiO_2@LDH nanocomposites could be a good candidate as a kind of reinforcement filler for the green tires.

Keywords Core–shell · SiO_2@LDH nanocomposites · Rubber composites · Green tires · Dispersity improved

1 Introduction

Rubber materials have been widely used in the automobile tire industry for their unique elasticity. To improve the performance of rubber materials, the main strategy in the elastic field is to filling the rubber matrix with nanoparticles [1–5]. In the past decades, carbon black as an effective reinforcing filler has been extensively applied in the tire. The performance of the rubber matrix has been remarkably enhanced by the incorporation of carbon black, especially the mechanical properties and wear resistance [6–8]. However, with the gradual depletion of the petroleum resources and the awareness of the public environmental protection, it is urgent to develop a new material to replace the oil-depended carbon black. The concept of 'green tire' was derived from the environmental friendly low-cost preparation and outstanding reinforcement of rubber matrix. Silica nanoparticles (SiO_2), considered as an excellent substitute for carbon black, has attracted the worldwide attention in the tire industry [9–14]. The rubber tread were endowed with the reinforced mechanical properties as well as the improved wet skid resistance and decreased rolling resistance by filling with SiO_2 nanoparticles composites. Considering the close correlation between the properties of tires and the safety of automobile travelling as well as the fuel consumption, the using of SiO_2 nanoparticles becomes a core research [11, 15–18]. Nevertheless, due to the nano level particle size and a mass of hydrophilic groups on the surface, the aggregation of SiO_2 nanoparticles is inevitable after filling in the rubber matrix which lead to the decline of comprehensive properties [19, 20]. The enhancement of the comprehensive performance of rubber composites, especially the

✉ Hong Zhu, Zhuho128@126.com; ✉ Fanghui Wang, fhwang@mail.buct.edu.cn | [1]State Key Laboratory of Chemical Resource Engineering, School of Science, Beijing University of Chemical Technology, Beijing 100029, People's Republic of China.

SN Applied Sciences (2019) 1:345 | https://doi.org/10.1007/s42452-019-0324-8

Received: 18 January 2019 / Accepted: 1 March 2019 / Published online: 15 March 2019

improvement of the dispersity of SiO_2 nanoparticles in the matrix has become the focus of recent researches.

Layered double hydroxides (LDHs), owing to the flexible adjustability and alternation of the bivalent and trivalent metal ions on the layers has become a kind of conspicuous two dimensional materials [21–26]. In the past few years, a number of reports on LDH-based rubber composites revealed the application potential of LDH in the elastomer. As previously reported, the rubber matrix was reinforced in mechanical properties and functionalized with other performance, such as vulcanization, optical properties, flame retardant and environmental friendliness [27–31]. However, LDH is rarely reported for the application in fabricating green tire tread composites. In recent years, endowing a tire with high wet skid resistance and low rolling resistance has become a crux to the manufacture of 'green tire' [32, 33]. It is still a problem for tire rubber composites to obtain both the high wet skid resistance and the low rolling resistance.

In our previous study, we have assembled the SiO_2 nanodots with MgAl-LDH [34]. Although the SiO_2 nanodots with minimal size and the advanced performance were obtained, the fussy preparation and the difficulty in the quantitative control of SiO_2 nanodots has restricted its further application. Here, the LDH nanosheets were in situ grown on the surface of the pre-prepared SiO_2 nanoparticles to obtain SiO_2@LDH nanocomposites and further incorporated into SSBR/BR rubber matrix to fabricate SiO_2@LDH–SSBR/BR composites (Scheme 1). A group of SiO_2@LDH nanocomposites with different ratio of SiO_2 and LDH were obtained with the same preparation process for further study of the optimal SiO_2/LDH ratio. In addition, the synergistic effect of two materials distinctly improved the dispersity of fillers and enhanced the comprehensive performance of SSBR/BR matrix. This research opened up a new application of SiO_2@LDH nanocomposites.

2 Experimental section

2.1 Materials

$Mg(NO_3)_2{\cdot}6H_2O$ and $Al(NO_3)_3{\cdot}9H_2O$ were obtained from Beijing Chemical Works Co., Ltd. Na_2CO_3 and NaOH were produced by Beijing Chemical Works. The sodium silicate ($Na_2O{\cdot}3.2SiO_2$, 27 wt%) that used for the preparation of silica in this work was manufactured by Beijing Linhengtai Trade Co., Ltd.. Sulphuric acid and citric acid were obtained from Shanghai Macklin Biochemical Co., Ltd.. SSBR (Buna VSL 5025-2HM, oil-extended) and BR (CB24) were purchased from Lanxess Chemical Industry Co., Ltd. (Germany). Commercial Zeosil 1165MP highly-dispersed nano-SiO_2 was purchased from Rhodia France (Qingdao, China). Bis(3-triethoxysilylpropyl)tetrasulfide (Si69) was produced by Nanjing Shuguang Chemical Group Co., Ltd.

2.2 Preparation of SiO_2 nanoparticles

Typically, sodium silicate was mixed with a certain of deionized water (v/v = 1:3) and the mixture was heated to 80 °C. Ethanol was added into sodium silicate solution for the nucleation of SiO_2 nanoparticles. After being

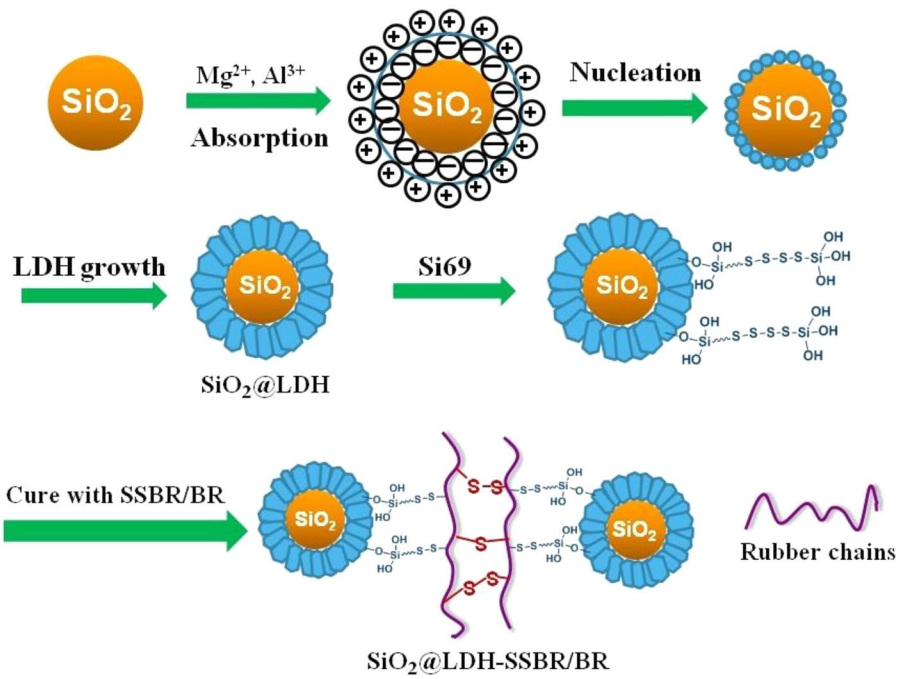

Scheme 1 Schematic preparation diagram of SiO_2@LDH and the fabrication of SSBR/BR composites

uniformly stirred, 7 mL citric acid (2.3 mol/L) was added into the sodium silicate solution. 2.5 mol/L H_2SO_4 solution was used to adjust the pH around 6. The silica mixture was aged for 6 h in ethanol. The SiO_2 mixture was washed by deionized water and dried at 60 °C overnight, then the pure SiO_2 nanoparticles was obtained. For comparison, the representative and outstanding commercialized Zeosil 1165MP highly-dispersed nano-SiO_2 was used in this study. According to our previous research, the SiO_2 nanoparticles prepared in Sect. 2.2 showed the similar mechanical properties and dispersity with the commercialized Zeosil 1165 MP in SSBR/BR, but the different dynamic mechanical properties [14, 34]. And the dynamic mechanical properties of SSBR/BR filled with two kinds of SiO_2 were studied particularly in Sect. 3.5 to highlight the performance of the SiO_2@LDH nanocomposites.

2.3 Preparation of SiO_2@LDH nanocomposites

Typically, 0.05 g SiO_2 nanoparticles that prepared in Sect. 2.2 was mixed with 20 mL deionized water, and then sonicated for 1 h. 0.1 g Na_2CO_3 was dissolved into the SiO_2 dispersion, forming solution A. 0.25 g $Mg(NO_3)_2{\cdot}6H_2O$ and 0.18 g $Al(NO_3)_3{\cdot}9H_2O$ were dissolved to form solution B. Then B was added slowly into A under a strong stirring. The pH of suspension was kept at 11 using 1 M NaOH, and uniformly stirred at room temperature. The mixture was washed 3 times with deionized water and ethanol respectively, and dried at 60 °C for 36 h to obtain SiO_2@LDH nanocomposites.

2.4 Preparation of SSBR/BR composites

Table 1 shows the mixing recipes of the SSBR/BR compounds. The method of the preparation of SSBR/BR composites refers to the previous studies of our group [14, 34].

2.5 Characterization

The morphologies of the nanocomposites were observed by a JEM-2100 transmission electron microscope (TEM). The fracture surface of the rubber composites was observed by an S-4800 scanning electron microscope (SEM). The crystalline structures of the nano materials samples were detected by an X-ray diffractometer (XD-3A, Japan). The surface elemental compositions of LDH, SiO_2 and SiO_2@LDH were measured by an X-ray photoelectron spectroscope (XPS) (Thermo Fisher LAB 250 ESCA System, USA).

The optimum vulcanized time (t_{90}) of the SSBR/BR composites was obtained using the MR-C3 moving-die rheometer (MDR) at 150 °C. The mechanical properties of vulcanizates were confirmed by a CTM4104 tensile tester (SANS, China). The dynamic rheological properties of the composites were measured by RPA2000 (Alpha Technologies Co., USA) at 60 °C and the strain amplitude was varied from 0.28 to 400% at the frequency of 1 Hz. Dynamic mechanical properties of the vulcanizates were tested by dynamic mechanical analysis (DMA) (VA3000, 01 dB-Metravib Co., Ltd., France). Test were set from − 80 to 80 °C under the condition of 3 Hz, and temperature rate was set as 3 °C/min.

Table 1 The compound formulation

Ingredient	Loading (phr)
SSBR	96.25
BR	30.00
ZnO	3.00
Stearic acid	1.00
SiO_2@LDH (Zeosil 1165MP)	70
Si69	10 wt% of filler
Accelerator D[a]	2.00
Accelerator CZ[b]	1.50
Antioxidant 4010NA[c]	1.50
Paraffin wax	1.00
Sulfur	1.40

Unit: Parts per hundred rubber, phr

[a]Accelerator D is 1,3-diphenylguanidine

[b]Accelerator CZ is *N*-cyclohexyl-2-beozothiazole sulfonamide

[c]Antioxidant 4010NA is *N*-isopropyl-*N*′-phenyl-1,4-phenylenediamin

3 Results and discussion

3.1 Morphology and structure

The TEM images displayed the morphology of prepared SiO_2 nanoparticles and SiO_2@LDH nanocomposites. In Fig. 1a, the particle size of prepared SiO_2 nanoparticles in Sect. 2.2 is about 15 nm on average. For SiO_2@LDH nanocomposites (Fig. 1b), the surfaces of SiO_2 nanoparticles are covered by a large quantity of sheet-like LDH and the particle size of SiO_2@LDH nanocomposites is about 40 nm (Fig. 1c). In addition, the isolated SiO_2 nanoparticles are hardly observed in the TEM image, indicating the high integration of the SiO_2@LDH nanocomposites. The dispersion state of the SiO_2@LDH nanocomposites were observed by SEM (Fig. 1d, e). The SiO_2@LDH nanocomposites are uniformly dispersed in the rubber matrix. Meanwhile, the sheet-like LDH can be observed in the fracture surface, suggesting that the gear-shaped SiO_2@LDH nanocomposites effectively prevent the rubber matrix

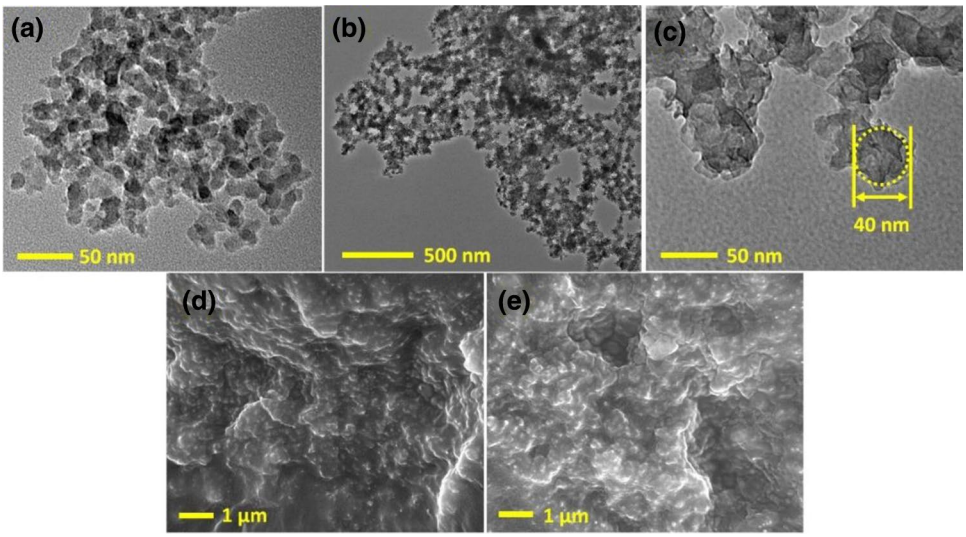

Fig. 1 TEM image of the prepared SiO_2 nanoparticles (**a**) and SiO_2@LDH nanocomposites with mass ratio of $M_{SiO_2} / M_{Mg(NO_3)_2 \cdot 6H_2O} = 5/2$ (**b**); Magnification of SiO_2@LDH nanocomposites (**c**); SEM images of the fracture surfaces of the vulcanizates with different mass ratio of $M_{SiO_2} / M_{Mg(NO_3)_2 \cdot 6H_2O} = 5/2$ (**d**) and 5/3 (**e**)

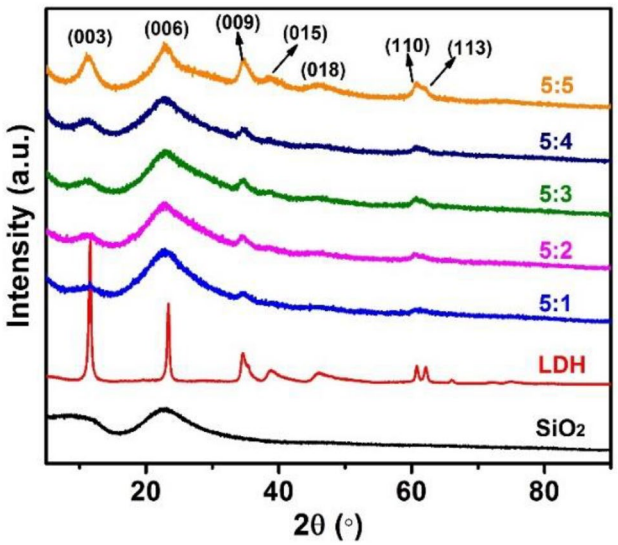

Fig. 2 XRD patterns of SiO_2, LDH and SiO_2@LDH with different mass ratio of $M_{SiO_2} / M_{Mg(NO_3)_2 \cdot 6H_2O}$

from disrupting and the mechanical properties of rubber composites are reinforced.

3.2 Chemical structure of characterization

The crystal structure of SiO_2 nanoparticles, LDH and different mass ratio of $M_{SiO_2} / M_{Mg(NO_3)_2 \cdot 6H_2O}$ of SiO_2@LDH are confirmed by the powder XRD. As shown in Fig. 2, the characterized diffraction of SiO_2 nanoparticles is presented at 22°, indicating the common amorphous structure of SiO_2 nanoparticles. For LDH, the characterized diffraction of (003), (006), (009), (015), (018), (110), and (113) appeared [35]. After the precipitation of LDH on the SiO_2 nanoparticles, the relative characterized diffraction occurred, indicating the combination of SiO_2 nanoparticles and LDH. Moreover, the intensity of the LDH peaks raised while the content of Mg^{2+} increased. Compared with LDH, the broadened diffractions of SiO_2@LDH are shown at the same 2θ positions, indicating that the LDH species is maintained in SiO_2@LDH [36]. Because the LDH species is diluted by SiO_2, the intensity of LDH species in SiO_2@LDH declined due to the combination of SiO_2 nanoparticles and LDH [34].

In order to investigate the interaction between SiO_2 nanoparticles and LDH nanosheets, the XPS of the sample was analyzed. The Mg 1*s*, O 1*s*, C 1*s*, Al 2*p*, Si 2*s* and Si 2*p* peaks are obviously shown in Fig. 3a, indicating the presence of Mg, Al, O, C and Si in the SiO_2@LDH nanocomposites. As shown in Fig. 3b, magnification of Si 2*p* electronic orbit spectrum can be deconvoluted into two kinds of Si^{4+} species fitting peaks: the SiO_2 and [SiO_4] tetrahedron [34, 37]. The presence of [SiO_4] tetrahedron proves the formation of new bonds between SiO_2 and LDH which could further confirms the hybridized structure within the SiO_2@LDH and the interaction between SiO_2 and LDH.

3.3 Dynamic rheological properties

Obviously, for each sample, the value of G′ decreased dramatically as shown in Fig. 4 because of the well-known 'Payne effect' [38, 39]. When the compounds are deformed by external stress, the filler–filler interaction and the value of G′ decrease gradually with the increasing of strain amplitude. Compared with SiO_2 nanoparticles, LDH shows a remarkable decreasing of G′ during the strain amplitude, indicating that the LDH forms a weaker filler network structure [35]. Notably, there are several new trends of G′ value are observed after filling with SiO_2@LDH. At the ratio of $M_{SiO_2} / M_{Mg(NO_3)_2 \cdot 6H_2O} = 5/1$, the G′ value of

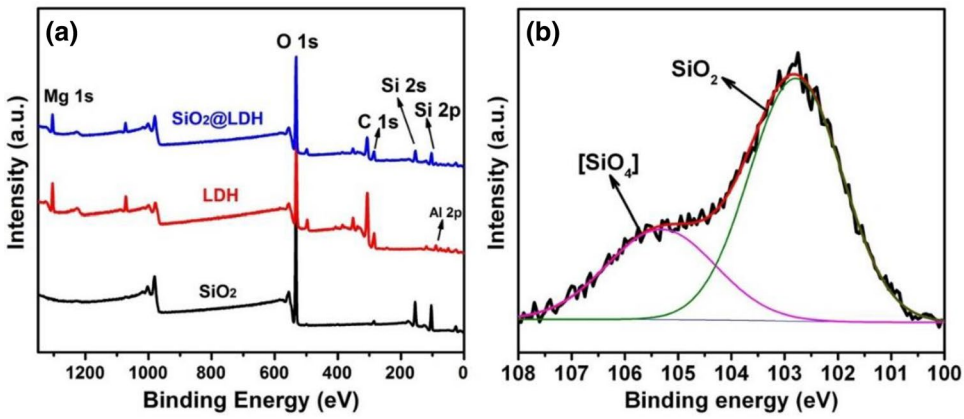

Fig. 3 XPS spectra: **a** survey spectra of SiO_2, LDH and SiO_2@LDH; **b** Si 2*p* spectra of SiO_2@LDH nanocomposites

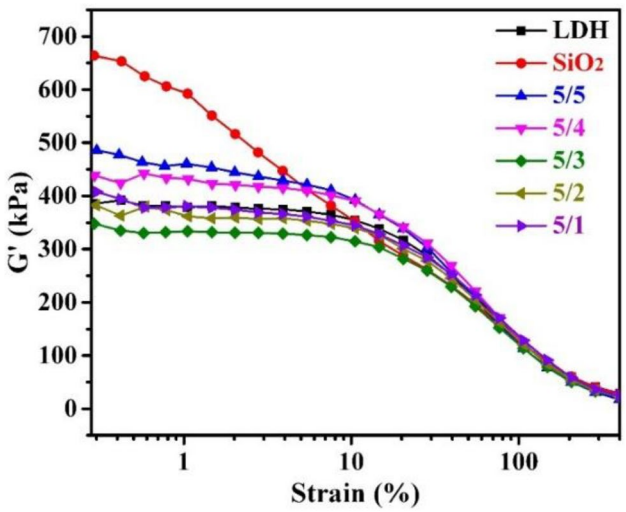

Fig. 4 Dependence of G′ of the LDH, SiO_2 and SiO_2@LDH on strain with different mass ratio of $M_{SiO_2} / M_{Mg(NO_3)_2 \cdot 6H_2O}$

SSBR/BR compound is dramatically decreased and almost closed to LDH–SSBR/BR, indicating that LDH acts as an important role in reducing the formation of filler network structure. With the increase of LDH content, the G′ values are decreased even lower than LDH–SSBR/BR at the ratio of $M_{SiO_2} / M_{Mg(NO_3)_2 \cdot 6H_2O} = 5/3$. This phenomenon can be explained by the morphology of the SiO_2@LDH nanocomposites. In SiO_2@LDH nanocomposites, the sheet-like LDH is grown vertically on the surface of SiO_2 nanoparticles, creating an initiative insulation from each other as observed in the TEM images. Furthermore, the sheet-like LDH shows weaker filler network structure compared with solely spherical SiO_2 nanoparticles, indicating the further decreasing of G′ values. With a further increasing of LDH content, the increscent size and the increasing number of LDH lead to the stack of LDH nanosheets and complicated filler network structure. Although the initial G′ values of SiO_2@LDH–SSBR/BR show an increasing trend, the initial G′ values are still at a relatively low level compared with SiO_2, indicating the combination of SiO_2 nanoparticles and LDH leads to the attenuation of the filler network structure.

3.4 Mechanical properties

SiO_2@LDH nanocomposites act as an important role to the mechanical properties of SSBR/BR composites. At 100% strain, the filler network structure has not been destroyed, the stress is mainly contributed by the filler network structure and the interaction of fillers. While increasing to 300% strain, the filler–rubber interaction mainly contributes to the stress since the filler network structure collapsed. In Fig. 5a, compared with SiO_2–SSBR/BR, the tensile modulus (300% strain) of SiO_2@LDH–SSBR/BR along with tensile strength increased, but the tensile modulus (100% strain) obviously decreased with the $M_{SiO_2} / M_{Mg(NO_3)_2 \cdot 6H_2O}$ ratio below 5/4. The decreasing of stress at 100% strain at low ratio of LDH further proved the increasing degree of dispersion after the assembly of SiO_2 and LDH. In addition, the raising of stress at 300% strain indicated that the increasing of chemical action between SiO_2@LDH and rubber matrix. Compared with SiO_2 nanoparticles, the SiO_2@LDH nanocomposites are more likely to react with Si69 due to the increasing number of reactive sites. The enhancement of elongation at break with the ration of $M_{SiO_2} / M_{Mg(NO_3)_2 \cdot 6H_2O} = 5/1$ is owing to the slippage of rubber chains on the oriented LDH layers [40]. At high content of LDH, although the number of reactive sites for single nanoparticle increased, the dramatically enlargement of particle size and the decline of dispersion of SiO_2@LDH nanocomposites dominate the decreasing of tensile strength.

In Fig. 5b, the LDH and SiO_2 nanoparticles show conspicuous enhancement in the elongation at break and the tensile strength. The SiO_2@LDH shows the obvious synergistic effect in the reinforcement of rubber matrix because

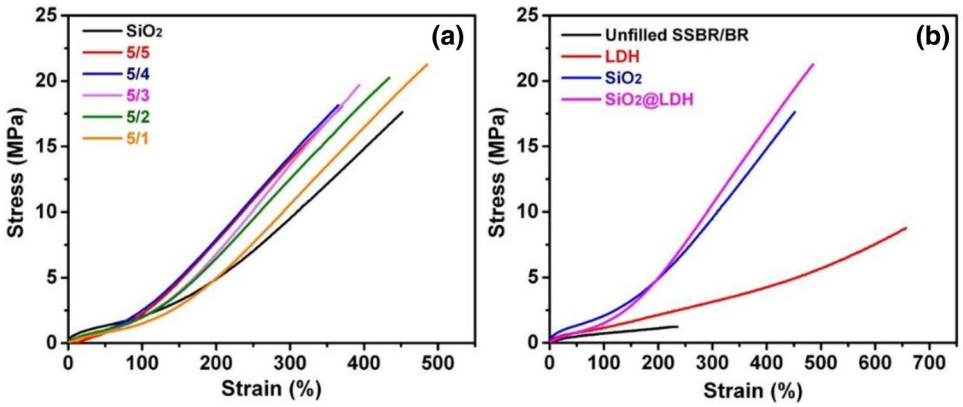

Fig. 5 **a** The true stress–strain curves of SiO_2@LDH–SSBR/BR composites; **b** the true stress–strain curves of SSBR/BR composites filled with different fillers

of the improving of dispersion and the increasing number of reactive sites. The aforementioned results clearly reveal that the mechanical properties is significantly enhanced by SiO_2@LDH.

3.5 Dynamic mechanical analysis

Dynamic mechanical analysis was used to further investigate the interaction between SiO_2@LDH nanocomposites and SSRB/BR matrix. Figure 6a, b show that the values of storage modulus (G′) dramatically decreased because of the energy dissipation during the glass–rubber transition of SSBR/BR as temperatures rise [41]. The values of G′ is highly related to the dispersity of fillers and filler–rubber interaction [42, 43]. Obviously, with the increasing content of LDH at low temperature range, the G′ values of SiO_2@LDH–SSBR/BR decrease at first and then raise. Below glass-transition temperature, the values of G′ are mostly contributed by filler–filler interaction due to the restriction of rubber chains [13]. So the decreasing of G′ indicating the decline of SiO_2@LDH network structure at low LDH content. At $M_{SiO_2} / M_{Mg(NO_3)_2 \cdot 6H_2O} = 5/5$, the increasing size and stack of LDH nanosheets mainly contribute the raise of G′. At high temperature range, with the increasing ratio of LDH, a more evident trend is observed at high temperature range, indicating the improved dispersity and enhanced filler–rubber interaction.

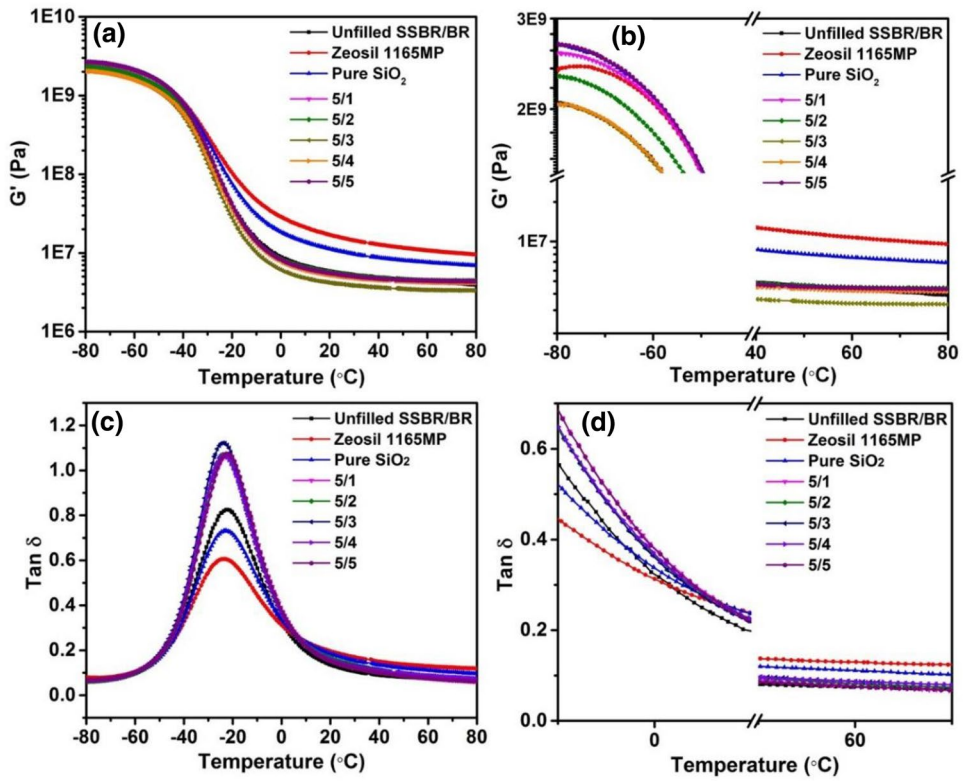

Fig. 6 **a** Dependence of storage modulus (G′) of different SSBR/BR composites on temperature; **b** enlargement of **a** at low and high temperature range; **c** dependence of tan δ of different SSBR/BR composites on temperature; **d** enlargement of **c** near 0 °C and 60 °C

Figure 6c, d show the dependence of tan δ of vulcanized rubber on different temperature. In Fig. 6c, the prepared SiO_2–SSBR/BR composites shows a higher value of tan δ than Zeosil 1165MP–SSBR/BR. Compared with two types of SiO_2–SSBR/BR composites, there are higher values of tan δ of the SiO_2@LDH–SSBR/BR composites with different ratio of $M_{SiO_2} / M_{Mg(NO_3)_2 \cdot 6H_2O}$. In the glass–rubber transition of SSBR/BR composites, the restriction of the movement of rubber chains is determined by the dispersion degree of fillers in rubber matrix and the energy dissipation is mostly caused by the friction between rubber chains. As a result, the improved dispersion of fillers in rubber matrix leading to an increased value of tan δ [44]. In addition, the effective volume of rubber chains also increased with the improving of fillers dispersion, leading to the rising number of unrestricted rubber chains and a high value of tan δ [45]. The results above suggest that the SiO_2@LDH nanocomposites possess a better degree of dispersion than SiO_2 nanoparticles.

Figure 6d is the magnified region of Fig. 6c near the temperature of 0 °C and 60 °C. As shown in Fig. 6d, compared with both types of SiO_2 in this experiment, all the SiO_2@LDH–SSBR/BR composites show higher tan δ values at 0 °C and lower tan δ values at 60 °C, indicating the enhanced wet skid resistance and decreased rolling resistance [7, 13, 46]. The vertically grown LDH nanosheets on the SiO_2 nanoparticle forms a hackly surface, and the interface of rubber-water can be easily broken. The tire is in firmly contacted with ground and provided high friction coefficient with the special serrated structure of the bare SiO_2@LDH nanocomposites. In addition, the hydrophilic group on the LDH accelerate a breaking of the rubber-water interface resulting to the enhancement of wet skid resistance. Tan δ value is depended on the collapse and reformation of the filler network structure at 60 °C [44, 47]. As discussed above, the SiO_2@LDH nanocomposites show high degree of dispersion in the elastomer, the friction between fillers decreased during cyclic deformation leading a decreasing of tan δ. Notably, although the more developed filler network structure is formed at the ratio of $M_{SiO_2} / M_{Mg(NO_3)_2 \cdot 6H_2O} = 5/4$ and 5/5, the values of tan δ are still lower than the SiO_2–SSBR/BR composites. The mobility and rotation of LDH are restricted due to the separation of SiO_2 nanoparticles, thus restrain the reformation of the filler network structure. We conclude that the comprehensive performance of SSBR/BR composites are effectively improved by SiO_2@LDH.

4 Conclusion

In this work, SiO_2@LDH nanocomposites were prepared by chemical assembly. The as prepared SiO_2@LDH were used in designing SSBR/BR compounds. The properties of SiO_2@LDH–SSBR/BR composites were studied. The characterizations of the SiO_2@LDH nanocomposites structures show a strong interaction between SiO_2 and LDH and the synergistic reinforcement effect in the SSBR/BR matrix. The investigation of the SiO_2@LDH–SSBR/BR properties reveals the improved dispersity of SiO_2@LDH and the reinforced filler–rubber interaction. The enhanced comprehensive performance of SSBR/BR matrix is obtained through the incorporation of SiO_2@LDH nanocomposites indicating a potential application in the green tires. This work may open up new opportunities to the development of SiO_2-based fillers for high-performance elastomer application.

Acknowledgements This work is supported by the National Basic Research Program of China (Grant Nos. 2015CB654700 and 2015CB654703), the National Natural Science Foundation of China (Nos. 21476020, 21776012 and 21776014), and the Joint Funds of the National Natural Science Foundation of China (No. U1705253).

Compliance with ethical standards

Conflicts of interest The authors declare that they have no competing financial interest.

References

1. Heinrich G, Klüppel M, Vilgis TA (2002) Reinforcement of elastomers. Curr Opin Solid State Mater Sci 6(3):195–203
2. Mora-Barrantes I, Ibarra L, Rodríguez A, Gonzalez L, Valentín JL (2011) Elastomer composites based on improved fumed silica and carbon black. Advantages of mixed reinforcing systems. J Mater Chem 21(43):17526–17533
3. Tadiello L, D'Arienzo M, Di Credico B et al (2015) The filler-rubber interface in styrene butadiene nanocomposites with anisotropic silica particles: morphology and dynamic properties. Soft Matter 11(20):4022–4033
4. Das A, Kasaliwal GR, Jurk R, Boldt R, Fischer D, Stöckelhuber KW, Heinrich G (2012) Rubber composites based on graphene nanoplatelets, expanded graphite, carbon nanotubes and their combination: a comparative study. Compos Sci Technol 72(16):1961–1967
5. Tang ZH, Zhang LQ, Feng WJ, Guo BC, Liu F, Jia DM (2014) Rational design of graphene surface chemistry for high-performance rubber/graphene composites. Macromolecules 47(24):8663–8673
6. Araby S, Meng QS, Zhang LQ, Zaman I, Majewski P, Ma J (2015) Elastomeric composites based on carbon nanomaterials. Nanotechnology 26(11):112001
7. Tang ZH, Zhang CF, Wei QY, Weng PJ, Guo BC (2016) Remarkably improving performance of carbon black-filled rubber composites by incorporating MoS_2 nanoplatelets. Compos Sci Technol 132:93–100

8. Du XY, Zhang YC, Pan XM, Meng FR, You JH, Wang ZF (2019) Preparation and properties of modified porous starch/carbon black/natural rubber composites. Compos Part B Eng 156:1–7
9. Chen LJ, Jia ZX, Tang YH, Wu LH, Luo YF, Jia DM (2017) Novel functional silica nanoparticles for rubber vulcanization and reinforcement. Compos Sci Technol 144:11–17
10. Zhong BC, Jia ZX, Luo YH, Jia DM (2015) A method to improve the mechanical performance of styrene–butadiene rubber via vulcanization accelerator modified silica. Compos Sci Technol 117:46–53
11. Stockelhuber KW, Svistkov AS, Pelevin AG, Heinrich G (2011) Impact of filler surface modification on large scale mechanics of styrene butadiene/silica rubber composites. Macromolecules 44(11):4366–4381
12. Li Y, Han BY, Liu L et al (2013) Surface modification of silica by two-step method and properties of solution styrene butadiene rubber (SSBR) nanocomposites filled with modified silica. Compos Sci Technol 88:69–75
13. Li Y, Han BY, Wen SP et al (2014) Effect of the temperature on the surface modification of silica and properties of modified silica filled rubber composites. Compos Part A Appl Sci Manuf 62:52–59
14. Kong LH, Li F, Wang FH, Miao Y, Huang XD, Zhu H, Lu YL (2018) High-performing multi-walled carbon nanotubes/silica nanocomposites for elastomer application. Compos Sci Technol 162:23–32
15. Meier JG, Fritzsche J, Guy L, Bomal Y, Klüppel M (2009) Relaxation dynamics of hydration water at activated silica interfaces in high-performance elastomer composites. Macromolecules 42(6):2127–2134
16. Gui Y, Zheng JC, Ye X, Han DL, Xi MM, Zhang LQ (2016) Preparation and performance of silica/SBR masterbatches with high silica loading by latex compounding method. Compos Part B Eng 85:130–139
17. Seo B, Kim H, Paik HJ, Kwag GH, Kim W (2013) Characterization of AN-SBR/Silica compound with acrylonitrile as a polar group in SBR. Macromol Res 21(7):738–746
18. Hall DE, Moreland JC (2001) Fundamentals of rolling resistance. Rubber Chem Technol 74(3):525–539
19. Yatsuyanagi F, Suzuki N, Ito M, Kaidou H (2001) Effects of secondary structure of fillers on the mechanical properties of silica filled rubber systems. Polymer 42(23):9523–9529
20. Ding Y, Yu ZH, Zheng JP (2017) Rational design of adhesion promoter for organic/inorganic composites. Compos Sci Technol 147:1–7
21. Fan GL, Li F, Evans DG, Duan X (2014) Catalytic applications of layered double hydroxides: recent advances and perspectives. Chem Soc Rev 43(20):7040–7066
22. Evans DG, Duan X (2006) Preparation of layered double hydroxides and their application as additives in polymers, as precursors to magnetic materials and in biology and medicine. Chem Commun 5:485–496
23. Zhao Y, Li F, Zhang R, Evans DG, Duan X (2002) Preparation of layered double hydroxide nanomaterials with uniform crystallite size using a new method involving separate nucleation and aging steps. Chem Mater 14(10):4286–4291
24. Wang XR, Lu J, Shi WY, Li F, Wei M, Evans DG, Duan X (2009) A thermochromic thin film based on host–guest interactions in a layered double hydroxide. Langmuir 26(2):1247–1253
25. Yang Y, Fan GL, Li F (2014) Synthesis of novel marigold-like carbonate-type Mg/Al layered double hydroxide micro-nanostructures via a two-step intercalation route. Mater Lett 116:203–205
26. Wang Q, O'Hare D (2012) Recent advances in the synthesis and application of layered double hydroxide (LDH) nanosheets. Chem Rev 112(7):4124–4155
27. Basu D, Das A, Stöckelhuber KW, Wagenknecht U, Heinrich G (2014) Advances in layered double hydroxide (LDH)-based elastomer composites. Prog Polym Sci 39(3):594–626
28. Pradhan B, Srivastava SK (2014) Layered double hydroxide/multiwalled carbon nanotube hybrids as reinforcing filler in silicon rubber. Compos Part A Appl Sci Manuf 56:290–299
29. Das A, Costa FR, Wagenknecht U, Heinrich G (2008) Nanocomposites based on chloroprene rubber: effect of chemical nature and organic modification of nanoclay on the vulcanizate properties. Eur Polym J 44(11):3456–3465
30. Acharya H, Srivastava SK, Bhowmick AK (2007) Synthesis of partially exfoliated EPDM/LDH nanocomposites by solution intercalation: structural characterization and properties. Compos Sci Technol 67(13):2807–2816
31. Das A, Wang D, Leuteritz A, Subramaniam K, Greenwell H, Wagenknecht W, Heinrich G (2011) Preparation of zinc oxide free, transparent rubber nanocomposites using a layered double hydroxide filler. J Mater Chem 21(20):7194–7200
32. Lin Y, Liu SQ, Peng J, Liu L (2016) The filler–rubber interface and reinforcement in styrene butadiene rubber composites with graphene/silica hybrids: a quantitative correlation with the constrained region. Compos Part A Appl Sci Manuf 86:19–30
33. Tunnicliffe LB, Thomas AG, Busfield JJC (2012) Silica–rubber microstructure visualised in three dimensions by focused ion beam–scanning electron microscopy. J Microsc 246(1):77–82
34. Kong LH, Li F, Wang FH, Miao Y, Huang XD, Zhu H, Lu YL (2018) In situ assembly of SiO_2 nanodots/layered double hydroxide nanocomposite for the reinforcement of solution-polymerized butadiene styrene rubber/butadiene rubber. Compos Sci Technol 158:9–18
35. Chen CP, Felton R, Buffet JC, O'Hare D (2015) Core–shell SiO_2@LDH with tuneable size, composition and morphology. Chem Commun 51(16):3462–3465
36. Yang DX, Song S, Zou YD et al (2017) Rational design and synthesis of monodispersed hierarchical SiO_2@layered double hydroxide nanocomposites for efficient removal of pollutants from aqueous solution. Chem Eng J 323:143–152
37. Li CJ, Lu H, Lin YY, Xie XL, Wang H, Wang LJ (2016) Self-sacrificial templating synthesis of self-assembly 3D layered double hydroxide nanosheets using nano-SiO_2 under facile conditions. RSC Adv 6(99):97237–97240
38. Wang MJ (1998) Effect of polymer–filler and filler–filler interactions on dynamic properties of filler vulcanizates. Rubber Chem Technol 71(3):520–589
39. Bokobza L (2004) The reinforcement of elastomeric networks by fillers. Macromol Mater Eng 289(7):607–621
40. Kotal M, Srivastava SK, Bhowmick AK (2010) Thermoplastic polyurethane and nitrile butadiene rubber blends with layered double hydroxide nanocomposites by solution blending. Polym Int 59(1):2–10
41. Bhattacharyya S, Sinturel C, Bahloul O, Saboung ML, Thomas S, Salvetat JP (2008) Improving reinforcement of natural rubber by networking of activated carbon nanotubes. Carbon 46(7):1037–1045
42. Kapgate BP, Das C (2014) Reinforcing efficiency and compatibilizing effect of sol–gel derived in situ silica for natural rubber/chloroprene rubber blends. RSC Adv 4(102):58816–58825
43. Zou YK, Sun YK, He JW, Tang ZH, Zhu LX, Luo YF, Liu F (2016) Enhancing mechanical properties of styrene–butadiene rubber/silica nanocomposites by in situ interfacial modification with a novel rare-earth complex. Compos Part A Appl Sci Manuf 87:297–309
44. Robertson CG, Lin CJ, Rackaitis M, Roland C (2008) Influence of particle size and polymer–filler coupling on viscoelastic glass transition of particle-reinforced polymer. Macromolecules 41(7):2727–2731
45. Wang M, Lu SX, Mahmud K (2015) Carbon–silica dual phase filler, a new generation reinforcing agent for rubber. Part vi. Time temperature superposition of dynamic properties of carbon–silica

dual phase filler filled vulcanizates. J Polym Sci Part B Polym Phys 38(9):1240–1249
46. Zeng ZQ, Yu HP, Wang QF, Lu G (2008) Effects of Coagulation processes on properties of epoxidized natural rubber. J Appl Polym Sci 109(3):1944–1949
47. Gopi JA, Patel SK, Chandra AK, Tripathy DK (2011) SBR-clay-carbon black hybrid nanocomposites for tire tread application. J Polym Res 18(6):1625–1634